

## Analysis of Extreme Rainfall in the Mt. Merapi Area

Anita Yuliana, Joko Sujono, Karlina\*

Department of Civil and Environmental Engineering, Universitas Gadjah Mada, Yogyakarta, INDONESIA  
 Jalan Grafika No 2 Yogyakarta

\*Corresponding author: [karlina.sipil@ugm.ac.id](mailto:karlina.sipil@ugm.ac.id)

SUBMITTED 04 October 2023 REVISED 01 December 2023 ACCEPTED 05 December 2023

**ABSTRACT** The slopes of Mount Merapi (Mt. Merapi) are an area prone to hydrological disasters due to elevation and orography. Hydrological disasters that have the potential to occur include floods, erosion, landslides, and drought which are closely related to extreme rainfall. Spatial and temporal variability of rainfall in mountainous areas requires rainfall data that can represent rainfall events. Therefore, this research aims to obtain the reliability of satellite rainfall data in the extreme rainfall indices. The CHIRPS, GPM-IMERG FINAL (IMERG-F) and GPM-IMERG LATE (IMERG-L) will be used in the reliability analysis of satellite-based rainfall compared to observed rainfall station. To validate satellite rain data, statistical criteria are utilized with parameters such as Correlation Coefficient (R), Root Mean Squared Error (RMSE), and Relative Bias (RB). Satellite-based rainfall estimates have a weak to moderate correlation (0.19 – 0.55), the RMSE value is relatively good (12.18 – 31.35 mm) and the observed bias tends to underestimate the estimated values. The capabilities of the IMERG-F, IMERG-L and CHIRPS satellites as alternative rainfall data in the Mt. Merapi area are quite good where IMERG-L has the best performance in capturing rainfall above 50 mm (R50mm), Consecutive Dry Days (CDD) indices, max 1-day and 5-day precipitation (Rx1day and Rx5day). The potential for extreme rainfall that is most prone to trigger lava floods occurs in the western region of Mt. Merapi at Ngandong Station (Sta. Ngandong). In this region, there is a high occurrence of extreme rainfall events. For instance, there were 501 instances of R50mm with an intensity of 77 mm day<sup>-1</sup>, Total Precipitation (PRCPTOT) reaches 3385 mm, Rx5day reaches 393 mm, and Consecutive Wet Days (CWD) lasts for 30 days. The results of this analysis can assist in climate understanding and modeling of extreme rainfall relevant to the region and support water resource management and disaster risk mitigation.

**KEYWORDS** Satellite-based Rainfall; Extreme Precipitation Indices; ETCCDI; IMERG; CHIRPS

© The Author(s) 2024. This article is distributed under a Creative Commons Attribution-ShareAlike 4.0 International license.

### 1 INTRODUCTION

The management of water is crucial for its multiple roles in sustaining life. It must be used wisely, controlled to prevent destruction, and conserved for future sustainability as mentioned in Water Resources Act (*Undang-undang Nomor 17 Tahun 2019 tentang Sumber Daya Air*, 2019). Rainfall is a significant aspect of the global water cycle, and heavy rainfall with an intensity of over 50 mm day<sup>-1</sup> can trigger extreme weather events, according to Meteorology, Climatology, and Geophysics Agency. Based on data from National Disaster Management Agency, in 2022, Indonesia faced 3,542 disaster events, and the frequency of such events can cause hydrological disasters such as floods, severe droughts, and tropical cyclones. This poses a high risk to the affected areas.

Rainfall varies spatially and temporally, and it requires evenly distributed measuring instruments

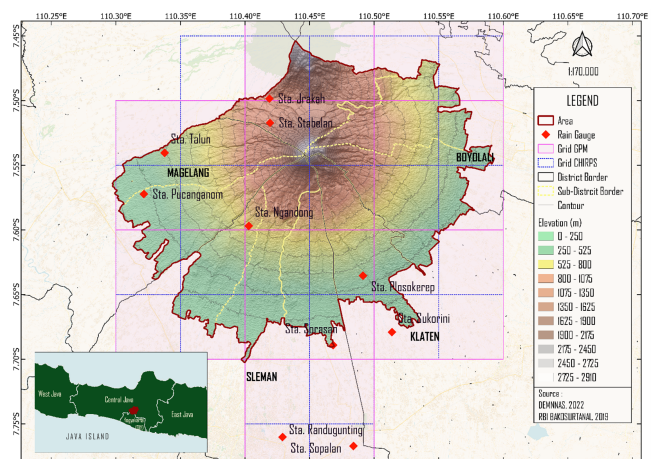


Figure 1 Map of research location

to collect adequate data in a region (Misnawati et al., 2018). However, some regions lack good quality and sufficient rainfall measurement data. In such cases, satellite-based rainfall data esti-

Table 1. Resolution of SPPs

|               | IMERG-F   | IMERG-L  | CHIRPS V02   |
|---------------|---|--|--|
| Dataset       | Integrated Multi-satellite Retrievals for GPM Final Run | Integrated Multi-satellite Retrievals for GPM Late Run | Climate Hazards group InfraRed Precipitation with Stations |
| Source        | NASA  | NASA   | CHC, UCB   |
| Spatial res.  | 0.1° ( $\pm$ 10 km)                                     | 0.1° ( $\pm$ 10 km)                                    | 0.05° ( $\pm$ 5 km)  |
| Temporal res. | Daily   | Daily  | Daily  |
| Availability  | 2000 - 2021   | 2000 - now   | 1981 - now   |
| Range         | 60°S - 60°N   | 60°S - 60°N  | 50°S - 50°N  |

mates are used, but recent comparisons reveal that no single dataset is consistently better in all rainfall parameters analyzed (Rauniyar et al., 2017).

Certain areas near Mt. Merapi are at risk for hydrological disasters due to elevation and orographics (Prayuda, 2012; Partiwati et al., 2012). The direction and speed of wind also have a significant impact on rainfall patterns on mountain slopes. Typically, slopes facing west experience higher rainfall compared to those facing east. Data on rainfall at Mt. Merapi shows that the higher the elevation, the more rainfall there is to the north and west, with maximum annual and daily rainfall recorded in these areas (Prayuda, 2015; Sofia, 2017). Daily rainfall tends to be higher at night and in the morning than during the day due to cooling (Rahmawati et al., 2021), which can trigger disaster events in the area.

Putra et al. (2019) conducted studies on alternative rainfall measurements in the Mt. Merapi region and found that measured rainfall data and radar have periods of NR (Not Recorded) data that can significantly affect disaster early warning systems. Satellites provide wider coverage of rainfall patterns and complete data lengths, making detecting rainy and dry days easier.

Research related to the extreme rainfall indices has been done before, but due to the many weaknesses of rain gauge data scattered in the Mt. Merapi area such as blank data or unrecorded data, this research is important to examine the use of satellite rain that is appropriate for use in the Mt. Merapi region that is able to represent the characteristics of extreme rain.

The aim of this study is to evaluate the ability of satellite rainfall, identify and assess the potential for extreme rainfall that can trigger natural disas-

Table 2. Value  $Q/\sqrt{n}$  and  $R/\sqrt{n}$  (Harto, 1993)

| n        | $Q/\sqrt{n}$ |      |      | $R/\sqrt{n}$ |      |      |
|----------|--------------|------|------|--------------|------|------|
|          | 90%          | 95%  | 99%  | 90%          | 95%  | 99%  |
| 10       | 1.05         | 1.14 | 1.29 | 1.21         | 1.28 | 1.38 |
| 20       | 1.10         | 1.22 | 1.42 | 1.34         | 1.43 | 1.60 |
| 30       | 1.12         | 1.24 | 1.46 | 1.40         | 1.50 | 1.70 |
| 40       | 1.13         | 1.26 | 1.50 | 1.42         | 1.53 | 1.74 |
| 50       | 1.14         | 1.27 | 1.52 | 1.44         | 1.55 | 1.78 |
| 100      | 1.17         | 1.29 | 1.55 | 1.50         | 1.62 | 1.86 |
| $\infty$ | 1.22         | 1.36 | 1.63 | 1.62         | 1.75 | 2.00 |

ters. This information will then be used to establish an early warning system for disaster events, which will serve as a scientific basis for decision makers. The analysis of extreme rainfall in the Mt. Merapi region will provide valuable insights for planning, disaster risk mitigation, and decision making, and will also help to improve the understanding of early warning systems for disaster risk.

## 2 METHODS

### 2.1 Location and Research Data

The study is located on the Mt. Merapi area, which is administratively between Klaten, Magelang, Boyolali and Sleman Regency (Figure 1). The data used in this study is secondary data, namely ground rainfall station was collected from official documents issued by Balai Teknik Sabo and Satellites Precipitation Products (SPPs).

Real-time global rainfall can be obtained through satellite-based rainfall by capturing microwave and infrared signals. These SPPs showers provide spatial continuity and consistency, making them useful for detecting uneven spatial distribution of observed rainfall (Liu et al., 2022). GPM-IMERG has high correlation with observed rainfall, tem-

poral and daily scale rainfall accumulation, light-moderate rainfall, able to detect days without rain (drought), and able to represent rain at low to moderate altitudes (Zhang et al., 2018; Liu et al., 2022). CHIRPS is best for describing wet periods, seasonal or monthly patterns (Ayehu et al., 2018; Wiwoho et al., 2021). According to Filho et al. (2022), IMERG-F and CHIRPS are better at capturing extreme rainfall compared to other rain satellites. Table 1 contains information on the SPPs used in this study.

## 2.2 Data Consistency Test

To ensure reliable rainfall data, it is necessary to conduct data reliability tests to verify that the obtained data comes from the same population and to assess the error rate of the ground station data (Yuono and Mulyandari, 2021). The Rescaled Adjusted Partial Sum (RAPS) method is more thorough as it does not rely on other station data as a reference. In the RAPS method, if the obtained value is smaller than the critical value for the year and the appropriate confidence level, then the data is considered reliable.

The reliability of rainfall data at stations around Mt. Merapi has previously been tested (Sapan et al., 2022). In this study, the time span of rainfall data analyzed is until 2022. Data consistency test can be calculated using the following equation (Harto, 1993).

$$S_0^* = 0 \quad (1)$$

$$S_k^* = \sum_{i=1}^k (Y_i - \bar{Y}), \text{ with } k = 1, 2, \dots, n \quad (2)$$

$$S_k^{**} = \frac{S_k^*}{D_y}, \text{ with } k = 1, 2, \dots, n \quad (3)$$

$$D_y^2 = \sum_{i=1}^n \frac{(Y_i - \bar{Y})^2}{n} \quad (4)$$

With  $n$  number of data  $Y$ ;  $Y_i$  annual rainfall value to  $-i$ ; average rating;  $S_k^*$  cumulative deviation value;  $S_k^{**}$  RAPS test value; and  $D_y$  standard deviation.

$$Q = \max |S_k^{**}|, 0 \leq k \leq n \quad (5)$$

$$R = \max S_k^{**} - \min S_k^{**}, 0 \leq k \leq n \quad (6)$$

The statistics that can be used as a tool to test their usefulness and the critique values  $Q$  and  $R$  are shown in Table 2.

## 2.3 Validation Test

To assess how accurately a model predicts hydrological processes, we use a process called validation. During this stage, we compare statistical indicators that measure the performance of SPPs against measured rainfall. These indicators include the  $R$ ,  $RMSE$ , and  $RB$ . The  $R$  value measures the linear relationship between SPPs and ground station data. It ranges from  $-1$  to  $1$ , with  $0$  indicating no correlation. The  $RMSE$  measures the magnitude of the mean absolute error between SPPs and surface rainfall data, where  $0$  is a perfect score.  $RB$  shows the SPPs bias. The optimal value for  $RB$  is  $0$ . A positive value indicates an overestimate of rainfall, while a negative value indicates an underestimate. We can represent these statistical parameters in an equation, as shown in Table 3.

## 2.4 Extreme Rainfall Indices

Experts from the Expert Team On Climate Change Detection and Indices (ETCCDI, [etccdi.pacificclimate.org/list\\_27\\_indices.shtml](http://etccdi.pacificclimate.org/list_27_indices.shtml)) have studied the extreme rainfall indices, which is calculated through frequency and intensity indicators using measured rainfall data. This indices is used to monitor extreme conditions, climate change, and aid in disaster mitigation. Sapan et al. (2022) conducted a study on the extreme rainfall indices in the Mt. Merapi area by examining the PRCPTOT indices and adding a review of the CDD, CWD, R50mm, Rx1day, and Rx5day indices. The extreme rainfall indices were calculated using Climact2 software, and Figure 2 developed by UNSW shows the display. Table 4 provides a further explanation.

## 3 RESULTS

### 3.1 Data Description

The description of the data period and recorded data is shown in Table 5. The accuracy of rainfall data plays a crucial role in the analysis process. Station data often contains a percentage of unrecorded data, ranging from  $5.3\%$  to  $52\%$ . This inconsistency in data loss or unrecorded data is a

Table 3. Summary of statistical parameters

| Statistical parameters         | Equation   | Range   | Optimum value | Source                                       |
|--------------------------------|--|---------|---------------|--|
| Correlation coefficient (R)    | $R = \frac{\sum_{i=1}^n (X_i - \bar{X})(Y_i - \bar{Y})}{\sqrt{\sum_{i=1}^n (X_i - \bar{X})^2 \sum_{i=1}^n (Y_i - \bar{Y})^2}}$ | [-1, 1] | 1             | (Pratiwi et al., 2020; Gustoro et al., 2022) |
| Root Mean Squared Error (RMSE) | $RMSE = \sqrt{\frac{\sum_{i=1}^n (X_i - Y_i)^2}{n}}$   | [0, ∞)  | 0             | (Hambali et al., 2019; Baig et al., 2022)    |
| Relative bias (RB)             | $RB = \frac{\sum_{i=1}^n (X_i - Y_i)}{\sum_{i=1}^n X_i} 100\%$   | (-∞, ∞) | 0             | (Gupta et al., 1999; Farzana et al., 2019)   |

where X observed rainfall; Y SPPs; and n amount of data.

Table 4. Extreme rainfall indices (WMO, 2023)

| Indices |                                   | Unit | Information   |
|---------|-----------------------------------|------|---|
| CDD     | Consecutive dry days              | day  | Maximum number of consecutive annual rainless days, $P \leq 1$ mm |
| CWD     | Consecutive wet days              | day  | Maximum number of consecutive annual rainy days, $P \geq 1$ mm    |
| R50mm   | Precipitation above 50mm          | day  | Number of annual rainy days, $P \geq 50$ mm                       |
| Rx1day  | Max 1 – day precipitation         | mm   | Maximum rainfall total for 1 day                                  |
| Rx5day  | Max 5 – day precipitation         | mm   | Maximum rainfall total over 5 days                                |
| PRCPTOT | Annual contribution from wet days | mm   | Total precipitation ( $P \geq 1$ mm)                              |

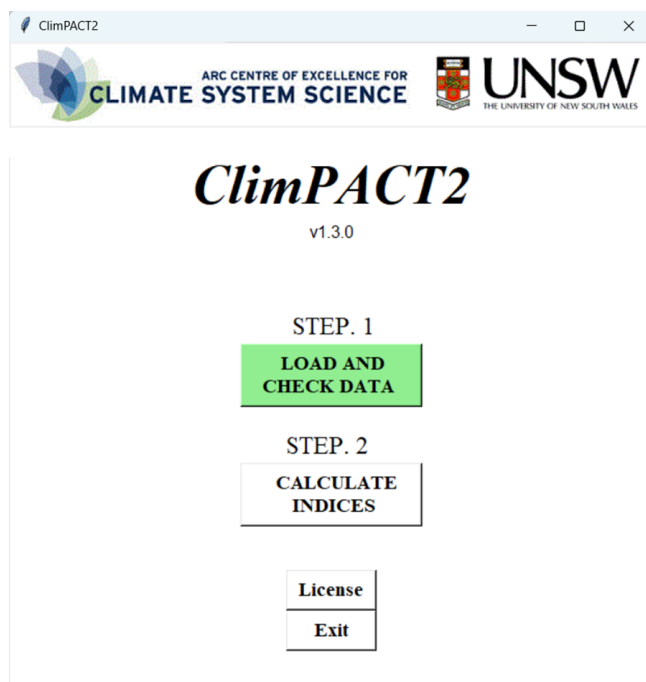


Figure 2 ClimPACT2 (WMO, 2016)

contributing factor to the use of SPPs in hydrological analyses.

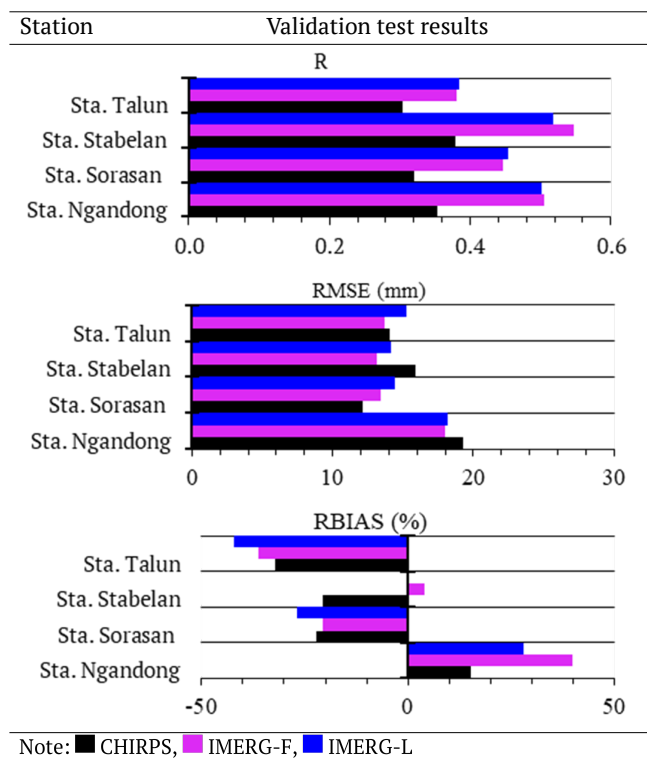
Table 5. Data period and data are not recorded (NR)

| Name              | Data period (Year) | Data NR (%) |
|-------------------|--------------------|-------------|
| Sta. Irakah       | 1980 – 2022        | 40.8 %      |
| Sta. Ngandong     | 1983 – 2022        | 52.1 %      |
| Sta. Plosokerep   | 1983 – 2022        | 41.1 %      |
| Sta. Pucanganom   | 1983 – 2022        | 40.3 %      |
| Sta. Randugunting | 1983 – 2022        | 11.9 %      |
| Sta. Sopalan      | 1986 – 2022        | 20.6 %      |
| Sta. Sorasan      | 1980 – 2022        | 5.3 %       |
| Sta. Talun        | 1980 – 2022        | 37.4 %      |
| Sta. Sukorini     | 1980 – 2022        | 37.7 %      |
| Sta. Stabelan     | 2014 – 2022        | 22.6 %      |
| CHIRPS            | 1981 – 2022        | 0 %         |
| IMERG-F           | 2000 – 2021        | 0 %         |
| IMERG-L           | 2000 – 2022        | 0 %         |

### 3.2 Data Consistency Test

We conducted data pruning tests using the RAPS method at SPPs and observed rainfall (CHIRPS, IMERG-F and IMERG-L) during each data period. After summarizing the data consistency test results, it was discovered that Irakah, Plosokerep, Randugunting, Sorasan, and Sukorini station had inconsistent data. Sorasan station represents the smallest percentage of NR in the southern Mount

Table 6. SPPs test results against observed rainfall



Merapi region, so it was included in the analysis. Sta. Pucanganom has consistent rainfall station data but was not used because the area is already represented by Sta. Talun, which has less unrecorded rainfall data. Sopalan and Randugunting Station were not used due to their long distance from the Mt. Merapi area. Therefore, the observed rainfall stations used in the analysis are Ngandong, Talun, Stabelan, and Sorasan Station.

On the other hand, all rainfall points matching the coordinates of the observed rainfall in SPPs had fixed data periods, which is illustrated in Figure 3. When the value obtained from Q and R test is greater than the value in Q and R table, the data is considered inconsistent.

### 3.3 Validation Test

The ability of SPPs to be validated based on the parameters R, RMSE and RBIAS is shown in Table 6 above. The results of the validation tests revealed that CHIRPS rainfall data had the weakest correlation to observations compared to IMERG-F and IMERG-L. The correlation between SPPs and observations only showed a weak to moderate correlation (0.30-0.55), which is because the analysis was done for daily rainfall. However,

the RMSE value was relatively good (12.18-19.26 mm), where CHIRPS performed better at Sta. Sorasan, while IMERG-F had a smaller error value at other stations. For RBIAS test results, CHIRPS had the smallest percentage of bias at Ngandong, and Talun Station. For IMERG-F, it had the smallest percentage of bias at Sta. Sorasan, and IMERG-L at Sta. Stabelan.

### 3.4 Extreme Rainfall Indices

Extreme rainfall indices, which includes R50mm, PRCPTOT, CDD, CWD, Rx1day and Rx5day were processed using Climact2 software within the RStudio application.

#### 3.4.1 R50mm Indices

Rainfall intensity above 50 mm, the extreme rainfall indices R50mm, is indicated as heavy rainfall according to BMKG and extreme rainfall according to WMO and is measured by the R50mm indices, as shown in Figure 4.

When analyzing the frequency distribution of rainfall events, it was found that the Sta. Ngandong had the highest frequency with 501 events, while the Sta. Stabelan had the lowest with only 80 events. The areas with the highest frequency of R50mm events were located around Mt. Merapi, which had a higher elevation and orographic influence. This information is supported by studies conducted by Prayuda (2015). The average heavy rainfall in the Sta. Ngandong was 77 mm, and the closest SPPs was IMERG-L due to its data distribution pattern and whisker resemblance. Similarly, in the Sta. Sorasan, the average heavy rainfall was 70 mm, and the closest SPPs was IMERG-F, which was able to capture the heavy rainfall in the area better than CHIRPS. In Sta. Stabelan, the average heavy rainfall was 72 mm, and the closest SPPs was IMERG-L. Finally, in the Sta. Talun, the average heavy rainfall was also 71 mm, and the closest SPPs distribution was IMERG-L.

#### 3.4.2 PRCPTOT Indices

One of the indices, PRCPTOT, indicates the amount of annual rainfall, as seen in Figure 5. According to the ground station, the southwest region of Mt. Merapi (Sta. Ngandong) experienced

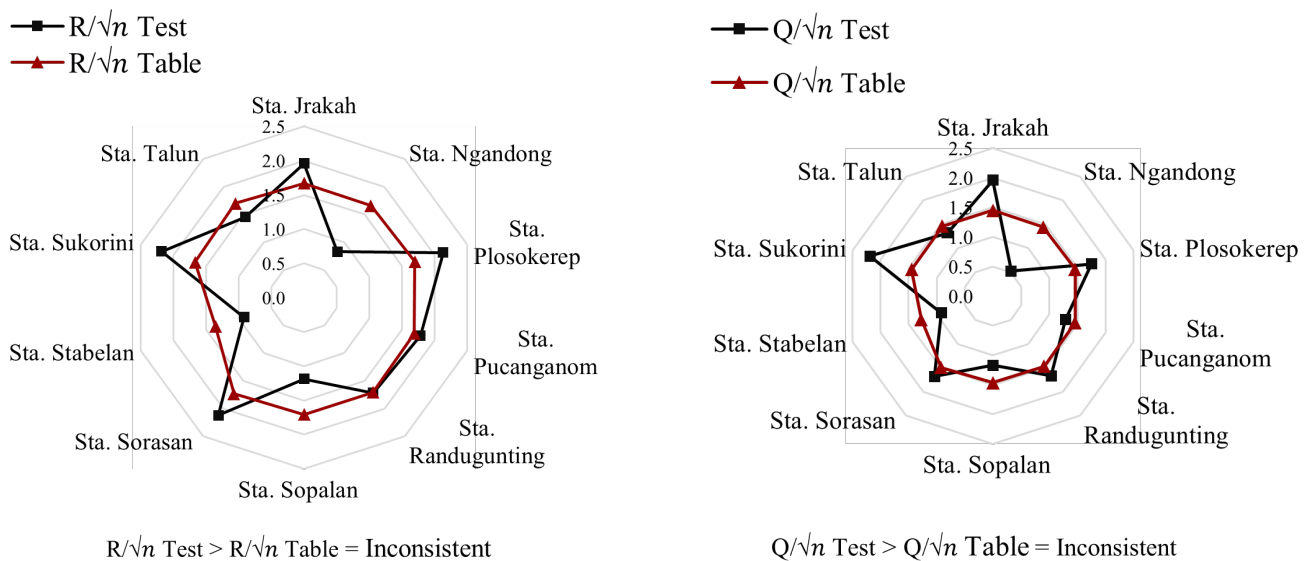


Figure 3 Results of the consistency test for observed rainfall based on critique values Q (a) and R (b).

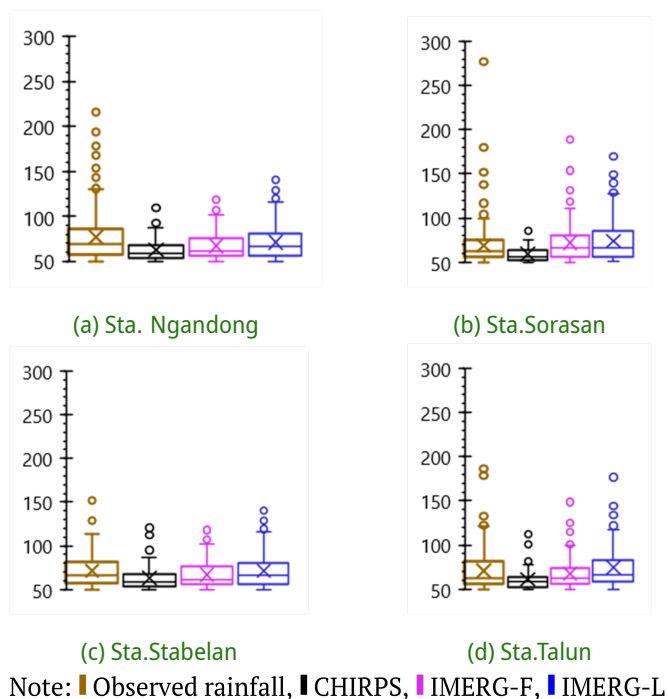


Figure 4 Rainfall intensity above 50 mm

the highest average annual rainfall at 3385 mm, while the northwest side (Sta. Stabelan) had an average of 2223 mm, the west region (Sta. Talun) had an average of 1920 mm, and the South region (Sta. Sorasan) had an average of 1757 mm. Although located in proximity, the weather stations experienced different indices due to orographic influences. In 2017 and 2019, the PRCPTOT indices

reflected the highest and lowest values.

The correlation in the scatter plot of monthly rainfall data is higher compared to annual rainfall data. This is because monthly data offers a higher time resolution, resulting in more data points and improving the accuracy of correlation estimates. Additionally, monthly data can reveal seasonal fluctuations and changes in rainfall patterns that occur throughout the year, while annual data combines all fluctuations into one number per year.

### 3.4.3 CDD, CWD, Rx1day and Rx5day Indices

Table 7 shows the extreme rainfall indices, including CDD, CWD, Rx1day, and Rx5day, as seen in the boxplot. The annual CDD indices indicate the number of consecutive days without significant rainfall (less than 1 mm) throughout the year. The longest CDD was observed at Sta. Stabelan with a duration of 60 days, while the shortest was at Sta. Ngandong with 39 days. IMERG-L is the closest in distribution to the CDD indices of the measuring station in terms of position, spread, and mean value. The annual CWD indices show the number of consecutive days with significant rainfall (greater than 1 mm) throughout the year. The longest CWD was observed at Sta. Ngandong with a duration of 17 days and a maximum of 30 days. The shortest was at Sta. Sorasan with a duration

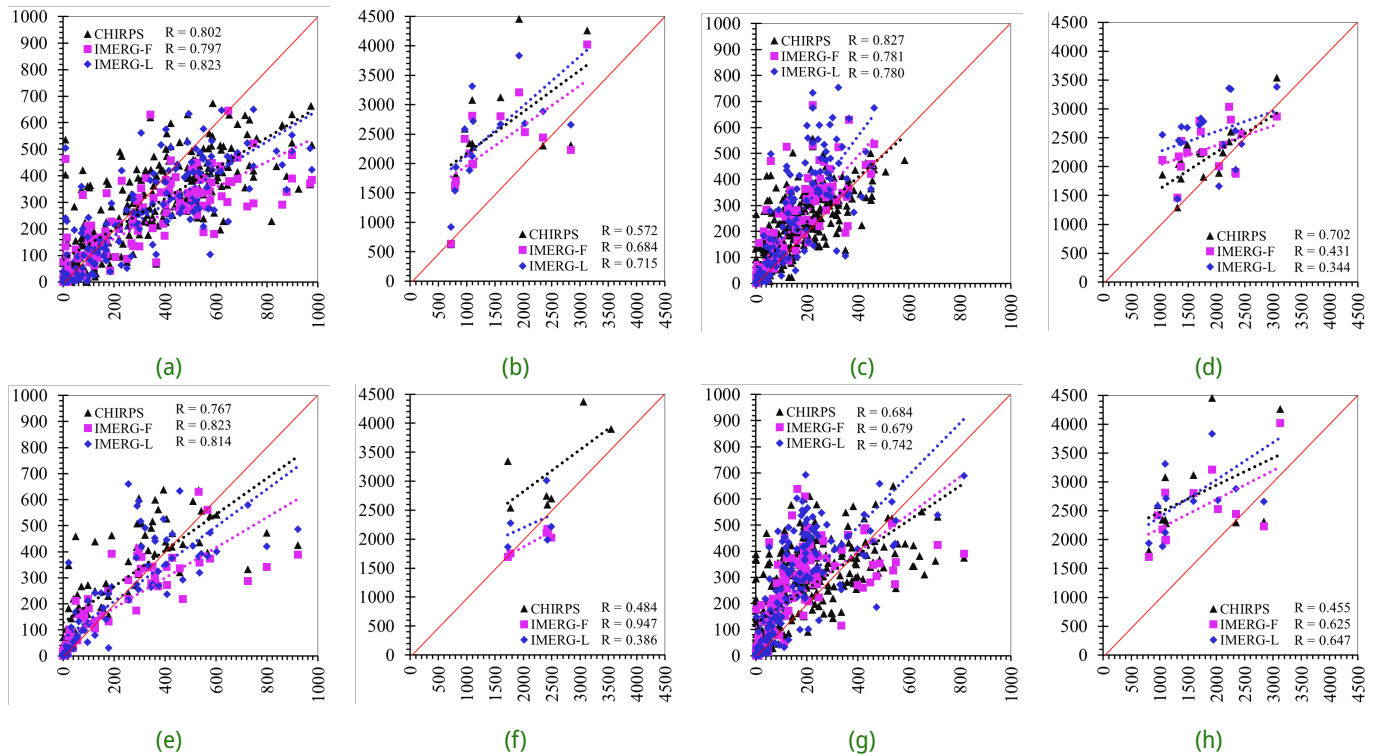


Figure 5 Scatterplot of satellite-based rainfall against observed rainfall (a) Sta. Ngandong monthly, (b) Sta. Ngandong annual, (c) Sta. Stabelan monthly, (d) Sta. Stabelan annual, (e) Sta. Sorasan monthly, (f) Sta. Sorasan annual, (g) Sta. Talun monthly, (h) Sta. Talun annual

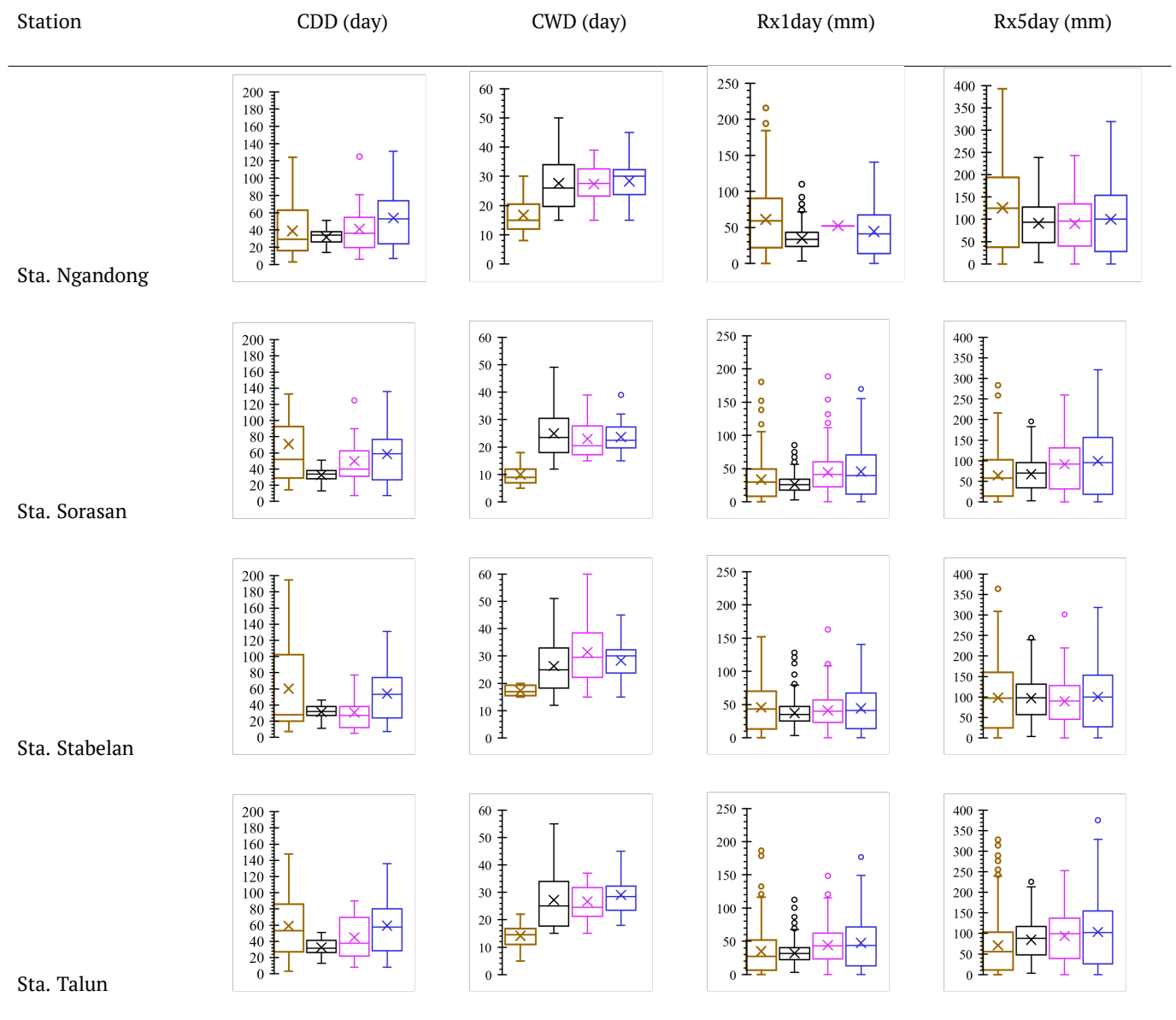
of only 10 days and a maximum of 18 days. Due to its sensitivity to light rainfall and spatial and temporal resolution, SPPs is not capable of providing detailed analysis of CDD and CWD indices. The Rx1day indices expresses the amount of daily extreme rainfall. The highest rainfall was recorded at Sta. Sorasan with a total of 277 mm, while CHIRPS, IMERG-F, and IMERG-L captured a maximum of 73 mm, 189 mm, and 170 mm of rain, respectively. The lowest rainfall was observed at Sta. Stabelan with a total of 152.2 mm, while CHIRPS, IMERG-F, and IMERG-L captured 112 mm, 91 mm, and 133 mm of rain, respectively. This indicates that the southern and western regions experience higher extreme rainfall. IMERG-L closely reflects the distribution of the Rx1day indices. The Rx5day indices have a greater intensity than Rx1day due to the cumulative value of extreme rainfall over five days. The highest 5 daily extreme rains were observed at Sta. Ngandong, with a maximum of 393 mm and an average of 126 mm. The lowest was at Sta. Sorasan, with a maximum intensity of 283 mm and an average of only 64 mm. Overall, SPPs has a good ability to capture the Rx5day extreme Rainfall indices.

#### 4 DISCUSSION

Based on the results described in Section 3, it is evident that some observed rainfall stations may provide unreliable rainfall data due to equipment malfunctions (such as ink jams, dead clocks, broken loggers, etc.) or natural disasters like the 2010 eruptions (Sandy Putra et al., 2012). It can be concluded that SPPs can provide reliable rainfall information with data classified as prevalent. The results of validation tests have shown that SPPs data has data that is able to represent surface rainfall. In general, SPPs that has better performance in the Mt. Merapi area is IMERG-L. This result is also supported by Talchabhadel et al. (2021) who examined the ability of several rain satellites to evaluate extreme rainfall in Nepal and found IMERG-LATE to be the best.

After conducting research, it was discovered that there were notable differences between the PRCP-TOT indices obtained from SPPs and the measurable rainfall data collected on the ground. The correlation between SPPs and observed rainfall yearly indicated a weak to strong relationship (0.118-0.897), while the correlation on a monthly scale was moderate to strong (0.457-0.678). CHIRPS

Table 7. Extreme rainfall indices



Note: ■ Observed rainfall, ■ CHIRPS, ■ IMERG-F, ■ IMERG-L

exhibited the weakest correlation across all four stations on a monthly scale, while IMERG-F performed exceptionally well at Sorasan and Stabelan Stations, and IMERG-L excelled at Talun and Ngandong Stations. On an annual scale, CHIRPS had the highest correlation at Sta. Sorasan, followed by IMERG-F at Sta. Stabelan and IMERG-L at Ngandong and Talun Stations. Spatially this station is not too far away but has a fairly different indices, this occurs due to orographic influences (Partiwi et al., 2012). These indices show the highest and lowest values in 2017 and 2019 which are visible on the PRCPTOT indices. Higher rainfall amounts are associated with floods and landslides,

while lower rainfall is associated with droughts and wildfires.

Overall, IMERG-L was the most effective in capturing rainfall above 50 mm, which is considered heavy rainfall by BMKG, while CHIRPS was less capable of representing heavy rainfall in both intensity and frequency. For extreme rainfall indices such as CDD, CWD, Rx1day and Rx5day, the most reliable satellite rainfall dataset was IMERG-L. Another study by Ramadhan et al. (2022) in Indonesia also suggests that IMERG-L is a better approximation for precipitation frequency, amount, duration, and intensity indices.

In this study, IMERG-L was found to be superior to other SPPs. This was also observed in a previous study by Tan and Santo (2018) in Malaysia, where IMERG-L had the least bias and overestimation compared to other datasets during flood periods. It is worth noting that satellite rainfall data does not account for orographic influences and differences in spatial resolution. This means that regions that are still within the same 1 spatial grid are considered to have the same rainfall characteristics, despite clear differences. Therefore, the use of SPPs in mountainous areas requires further analysis to address the effects of orography and spatial resolution. This is in line with research at Brantas Watershed by Wiwoho et al. (2021) which also explained that errors from SPPs are generally related to slope, wind, altitude, and evapotranspiration.

## 5 CONCLUSION

The analysis of extreme rainfall indices (CDD, CWD, Rx1day, Rx5day, PRCPTOT) in the Mt. Merapi region involves a comparison between measured rainfall data from stations and satellite rainfall data (CHIRPS, IMERG-F, and IMERG-L) for approximately 40 years from 1980 to 2022. SPPs estimates have a weak to moderate correlation (0.19 – 0.55), the RMSE value is relatively good (12.18 – 31.35 mm) and the observed bias tends to underestimate the estimated values, this occurs because the analysis is conducted on daily-scale rainfall data. Overall, all three satellite rainfall datasets can capture extreme rainfall intensity indices (R50mm, CDD, Rx1day, Rx5day, and PRCPTOT) effectively. The SPPs capabilities of CHIRPS, IMERG-F, and IMERG-L as alternative rainfall data in the Mt. Merapi region are quite good, with IMERG-L performing the best in capturing rainfall above 50 mm, CDD, Rx1day, and Rx5day indices, followed by IMERG-F and, lastly, CHIRPS. The region most vulnerable to triggering lahars due to extreme rainfall is in the western part of Mt. Merapi (Sta. Ngandong), where extreme rainfall indices (R50mm), PRCPTOT, Rx5day, and CWD are very high (77 mm with a frequency of up to 501 events, 3385 mm, 393 mm). The results of this analysis can contribute to a better understanding of the climate and modeling of extreme rainfall relevant to the region, supporting water resource management and disaster risk mitigation efforts

This, in turn, can aid in water resource management and disaster risk mitigation efforts. For instance, it can support hydrology analysis, water availability analysis required for irrigation and raw water needs, as well as provide valuable data input for the early warning system. The real-time results of this analysis are reliable and proven to be effective.

## DISCLAIMER

The authors declare no conflict of interest.

## ACKNOWLEDGMENTS

This study was supported and funded by Final Project Recognition Grant Universitas Gadjah Mada Number 5075/UN1.P.II/Dit-Lit/PT.01.01/2023. The authors appreciate the Balai Teknik Sabo for providing the data for this study especially for Santosa Sandy Putra, S.T., M.Sc. Ph.D who has guided the authors in this study.

## APPENDIX A. SUPPLEMENTARY DATA

Supplementary material related to this article can be found, in the online version, at [https://drive.google.com/drive/folders/116LJfFV\\_K\\_sj1qxLo5gE1wnupVqye-DuY?usp=sharing](https://drive.google.com/drive/folders/116LJfFV_K_sj1qxLo5gE1wnupVqye-DuY?usp=sharing)

## REFERENCES

- Ayehu, G. T., Tadesse, T., Gessesse, B. and Dinku, T. (2018), 'Validation of new satellite rainfall products over the Upper Blue Nile Basin, Ethiopia', *Atmospheric Measurement Techniques* **11**(4), 1921–1936.  
**URL:** <https://doi.org/10.5194/amt-11-1921-2018>
- Baig, F., Abrar, M., Chen, H. and Sherif, M. (2022), 'Rainfall consistency, variability, and concentration over the uae: Satellite precipitation products vs. rain gauge observations', *Remote Sensing* **14**(22), 1–26.  
**URL:** <https://doi.org/10.3390/rs14225827>
- Farzana, S. Z., Zafor, M. A. and Shahariar, J. A. (2019), 'Application of swat model for assessing water availability in Surma River basin', *Journal of*

*the Civil Engineering Forum* 5(1), 29.

**URL:** <https://doi.org/10.22146/jcef.39191>

Filho, G. M. R., Hugo Rabelo Coelho, V., da Silva Freitas, E., Xuan, Y., Brocca, L. and das Neves Almeida, C. (2022), 'Regional-scale evaluation of 14 satellite-based precipitation products in characterising extreme events and delineating rainfall thresholds for flood hazards', *Atmospheric Research* 276(May), 106259.

**URL:** <https://doi.org/10.1016/j.atmosres.2022.106259>

Gupta, H. V., Sorooshian, S. and Yapo, P. O. (1999), 'Status of automatic calibration for hydrologic models: Comparison with multilevel expert calibration', *Journal of Hydrologic Engineering* 4(2), 135–143.

**URL:** [https://doi.org/10.1061/\(asce\)1084-0699\(1999\)4:2\(135\)](https://doi.org/10.1061/(asce)1084-0699(1999)4:2(135))

Gustoro, D., Sujono, J. and Karlina (2022), 'Perbandingan pola distribusi hujan terukur dan hujan satelit di DAS Progo', *Jurnal Teknik Pengairan: Journal of Water Resources Engineering* 2022(1), 23–35.

**URL:** <https://doi.org/10.21776/ub.pengairan.2022.013.01.03>

Hambali, R., Legono, D. and Jayadi, R. (2019), 'Correcting radar rainfall estimates based on ground elevation function', *Journal of the Civil Engineering Forum* 5(3), 300.

**URL:** <https://doi.org/10.22146/jcef.49395>

Harto, S. (1993), *Analisis hidrologi*, Penerbit PT Gramedia Pustaka Utama.

Liu, S., Wang, J. and Wang, H. (2022), 'Assessing 10 satellite precipitation products in capturing the July 2021 extreme heavy rain in Henan, China', *Journal of Meteorological Research* 36(5), 798–808.

**URL:** <https://doi.org/10.1007/s13351-022-2053-y>

Misnawati, M., Boer, R., June, T. and Faqih, A. (2018), 'Perbandingan metodologi koreksi bias data curah hujan chirps', *Limnotek: perairan darat tropis di Indonesia* 25(1).

Partiwi, E. P., Sujono, J. and Jayadi, R. (2012), 'Kajian variabilitas curah hujan di kawasan lereng Gunung Merapi dengan uji mann-kendall', 13(1), 28–38.

**URL:** <https://doi.org/10.36706/jhs.v13i1.17>

Pratiwi, E. P. A., Ramadhani, E. L., Nurrochmad, F. and Legono, D. (2020), 'The impacts of flood and drought on food security in central java', *Journal of the Civil Engineering Forum* 6(1), 69.

**URL:** <https://doi.org/10.22146/jcef.51872>

Prayuda, D. D. (2012), 'Temporal and spatial analysis of extreme rainfall on the slope area of Mt. Merapi', *Civil Engineering Forum* XXI, 1285–1290.

**URL:** <https://doi.org/10.22146/jcef.18922>

Prayuda, D. D. (2015), 'Analisis karakteristik intensitas hujan di wilayah lereng Gunung Merapi', *Jurnal Rekayasa Infrastruktur* 1, 14–19.

**URL:** <https://doi.org/10.30607/jri.v1i1.52>

Putra, S. S., Ridwan, B. W., Yamanoi, K., Shimomura, M., Sulistiyani and Hadiyuwono, D. (2019), 'Point-based rainfall intensity information system in Mt. Merapi area by x-band radar', *Journal of Disaster Research* 14(1), 80–89.

**URL:** <https://doi.org/10.20965/JDR.2019.P0080>

Rahmawati, N., Rahayu, K. and Yuliasari, S. T. (2021), 'Performance of daily satellite-based rainfall in groundwater basin of merapi aquifer system, Yogyakarta', *Theoretical and Applied Climatology*.

**URL:** <https://doi.org/10.1007/s00704-021-03731-9>

Ramadhan, R., Muharsyah, R., Marzuki, Yusnaini, H., Vonnisa, M., Hashiguchi, H., Suryanto, W. and Sholihun (2022), 'Evaluation of gpm imerg products for extreme precipitation over Indonesia', *Journal of Physics: Conference Series* 2309(1).

**URL:** <https://doi.org/10.1088/1742-6596/2309/1/012008>

Rauniyar, S. P., Protat, A. and Kanamori, H. (2017), 'Uncertainties in trmm-era multisatellite-based tropical rainfall estimates over the maritime continent', *Earth and Space Science* 4(5), 275–302.

**URL:** <https://doi.org/10.1002/2017EA000279>

Sandy Putra, S., Hassan, C. and Hariyadi, S. (2012), 'Hot pyroclastic deposit as lahar resistor: A case study of gendol river after the Mt. Merapi 2010 eruption', *WIT Transactions on Engineering Sciences* 73, 97–109.

**URL:** <https://doi.org/10.2495/DEB120091>

Sapan, E. G. A., Sujono, J. and Karlina (2022), 'Analisis karakteristik hujan ekstrim menggunakan model iklim di wilayah Gunung Merapi', *Media Komunikasi Teknik Sipil* 28(1), 99–108.

**URL:** <https://doi.org/mkts.v28i1.36332>

Sofia, D. A. (2017), 'Analisis durasi hujan dominan dan pola distribusi curah hujan jam-jaman di wilayah Gunung Merapi', *Jurnal Teknologi Rekayasa* **1**(1), 7.

**URL:** <https://doi.org/10.31544/jtera.v1.i1.2016.7-14>

Talchabhadel, R., Nakagawa, H., Kawaike, K., Yamanoi, K., Musumari, H., Adhikari, T. R. and Prapapati, R. (2021), 'Appraising the potential of using satellite-based rainfall estimates for evaluating extreme precipitation: A case study of august 2014 event across the West Rapti River Basin, Nepal', *Earth and Space Science* **8**(8), 1–15.

**URL:** <https://doi.org/10.1029/2020EA001518>

Tan, M. L. and Santo, H. (2018), 'Comparison of gpm imerg, tmpa 3b42 and persiann-cdr satellite precipitation products over Malaysia', *Atmospheric Research* **202**(November 2017), 63–76.

**URL:** <https://doi.org/10.1016/j.atmosres.2017.11.006>

*Undang-undang Nomor 17 Tahun 2019 tentang*

*Sumber Daya Air* (2019).

Wiwoho, B. S., Astuti, I. S., Alfarizi, I. A. G. and Sucahyo, H. R. (2021), 'Validation of three daily satellite rainfall products in a humid tropic watershed, brantas, indonesia: Implications to land characteristics and hydrological modelling', *Hydrology* **8**(4).

**URL:** <https://doi.org/10.3390/hydrology8040154>

Yuono, T. and Mulyandari, E. (2021), 'Kajian penggunaan data hujan satelit trmm untuk perencanaan talang air irigasi pada Daerah Irigasi Ngarum', *Jurnal Teknik Sipil dan Arsitektur* **26**(1), 41–48.

**URL:** <https://doi.org/10.36728/jtsa.v26i1.1243>

Zhang, C., Chen, X., Shao, H., Chen, S., Liu, T., Chen, C., Ding, Q. and Du, H. (2018), 'Evaluation and intercomparison of high-resolution satellite precipitation estimates - gpm, trmm, and cmorph in the Tianshan Mountain Area', *Remote Sensing* **10**(10).

**URL:** <https://doi.org/10.3390/rs10101543>

[This page is intentionally left blank]